European Journal of Pharmaceutics and Biopharmaceutics 212 (2025) 114737

Contents lists available at ScienceDirect

European Journal of Pharmaceutics and Biopharmaceutics

journal homepage: www.elsevier.com/locate/ejpb

Research paper

Metallomic evaluation of selenium nanoparticles and selenomethionine for the attenuation of cisplatin-induced nephrotoxicity

Alejandro Iglesias-Jiménez, Gema Artiaga, Estefanía Moreno-Gordaliza, M. Milagros Gómez-Gómez *

Department of Analytical Chemistry, Faculty of Chemical Sciences, Universidad Complutense de Madrid, Avenida Complutense s/n, 28040 Madrid, Spain

ARTICLE INFO

Keywords:
Selenium nanoparticles
Selenomethionine
Cisplatin
Nephroprotection
Mass spectrometry
Chromatography

ABSTRACT

Nephrotoxicity is one of the most limiting side effects in oncologic patients treated with cisplatin and is still clinically unresolved. In this work, chitosan-stabilised selenium nanoparticles (Ch-SeNPs) and selenomethionine (SeMet) have been evaluated as nephroprotectors of cisplatin using renal proximal tubule epithelial cells (RPTEC/TERT1) as a model. Moreover, the antineoplastic efficacy of cisplatin co-administered with these selenocompounds has been tested in cervical cancer cells (HeLa). Cell viability, cell localisation of Ch-SeNPs and changes in the morphology and cell ultrastructure, Pt and Se cellular internalisation and cisplatin binding to DNA, and speciation of Pt and Se in the cytosolic extracts were evaluated by MTT assays, transmission electron microscopy coupled to energy dispersive X-ray spectroscopy (TEM-EDS), inductively coupled plasma mass spectrometry (ICP-MS), and both size exclusion chromatography (SEC) and anion exchange chromatography (AEC) coupled to either ICP-MS or UV–Vis. Differences in the pharmacological activity of the two selenospecies were observed. SeMet exerted a moderate protection on kidney cells while reducing their degree of cisplatin intracellular accumulation and DNA binding in both cell lines, but the antitumour effect of cisplatin was not significantly altered. Conversely, Ch-SeNPs did not impair the Pt-drug uptake or DNA binding in any cell type; and even increased its antitumour effect, which might enable using lower doses of cisplatin without loss of anticancer efficacy, which would result in decreased risk of renotoxicity. Furthermore, cells incubated either with SeMet or SeNPs showed higher levels of selenoproteins, which might enhance cellular defences against the reactive oxygen species (ROS) involved in cisplatin renotoxicity. Hence, both selenocompounds are envisioned as potential coadjuvants to reduce the risk of kidney impairment in future treatments with cisplatin.

1. Introduction

One of the current challenges in oncology research is focused on the improvement of chemotherapy based on cisplatin (*cis*-diamminedichloridoplatinum(II)), which exerts a cytotoxic effect based on the formation of crosslinked DNA-Pt adducts, being effective against a wide number of solid tumours [1,2]. However, diverse side effects may be developed, being renal toxicity the most treatment-limiting factor. In fact, around 30 % of cisplatin-treated patients end up presenting acute kidney injury, which forces the interruption of the therapy [3]. The problem originates when the drug is excreted through urine resulting from renal blood filtration [2]. Pt mainly accumulates in kidneys during this process, causing renal damage which especially affects epithelial cells of S-3 segment of the renal proximal tubules [4–6].

Different alternatives have been assayed in the last decades to avoid or ameliorate cisplatin-induced nephrotoxicity and enhance its clinical efficacy. Second and third generation Pt(II)-based drugs were developed, such as carboplatin, oxaliplatin, picoplatin, satraplatin, nedaplatin, lobaplatin or heptaplatin. More recently, polynuclear Pt(II) complexes, Pt(IV) prodrugs or nanosystems for delivery of Pt-drugs have been developed as well. However, only carboplatin and oxaliplatin have been approved worldwide for clinical use, and cisplatin is still irreplaceable for the treatment of several types of tumours [1,7]. On the other hand, numerous potential nephroprotective agents have been evaluated, not only considering their protective effect, but also the preservation of the antineoplastic effect of the Pt-drug [8,9]. However, none of the different tested agents have been yet approved for clinical use [10].

* Corresponding author.
E-mail addresses: alejandroiglesias@ucm.es (A. Iglesias-Jiménez), gmaayuso@ucm.es (G. Artiaga), emorenog@ucm.es (E. Moreno-Gordaliza), mmgomez@ucm.es (M. Milagros Gómez-Gómez).

https://doi.org/10.1016/j.ejpb.2025.114737
Received 28 October 2024; Received in revised form 23 April 2025; Accepted 6 May 2025
Available online 8 May 2025

Several selenocompounds have been tested as nephroprotectors, taking advantage of their antioxidant properties. A protective effect was observed when selenomethionine (SeMet) was co-administered with cisplatin in mice and rats, due to the formation of a Se-Pt complex between these compounds, leading to a decrease in the amount of DNA–cisplatin adducts in kidney [11,12]. More recently, selenium nanoparticles (SeNPs) are gaining increasing interest for biomedical research especially due to their potential for antitumour, antibacterial and antifungal applications [13–15]. The employment of capping agents provides SeNPs with higher stability and lower diameters, facilitating their cellular internalization [14–16]. Moreover, functionalized SeNPs have also been tested as vehicles for drug delivery and cellular detoxification, including nephroprotection during cisplatin treatment [13,15].

In this work, the potential of two Se species −chitosan-stabilized SeNPs (Ch-SeNPs) and SeMet- as nephroprotective agents for cisplatin therapies, has been evaluated using two different cell lines as a model for renal and cancer cells: human telomerase reverse transcriptase-immortalised renal proximal tubular epithelial cells (RPTEC/TERT1) and human cervical carcinoma cells (HeLa). Se and Pt metallomics studies were also performed to determine their correlation with the biological effects observed in the in vitro models.

2. Materials and methods

2.1. Standards and reagents

All solutions were prepared with ultrapure water obtained with a Milli-Q water purification system (Merck Millipore, Bedford, MA, USA), unless otherwise stated. All the chemicals and solvents employed were of analytical grade. Cisplatin, sodium selenite, sodium selenate, DL-selenomethionine (SeMet), seleno-L-cystine ($(SeCys)_2$) and seleno-(methyl)selenocysteine (MeSeCys) hydrochloride were purchased from Sigma-Aldrich (St. Louis, MO, USA). For the synthesis of SeNPs and the preparation of cisplatin solutions, ascorbic acid (Scharlab, Barcelona, Spain), deacetylated chitosan from shrimp shells (Sigma-Aldrich, St. Louis, MO, USA), glacial acetic acid and sodium chloride (Panreac AppliChem, Barcelona, Spain) were employed. Nitric acid (65 %, Scharlab, Barcelona, Spain) and hydrogen peroxide (33 %, Panreac AppliChem, Barcelona, Spain) were used for digestions of nanoparticles and cell pellets. Triton X-100 (Sigma-Aldrich), tris-(hydroxymetyl)-aminomethane (Tris) (Sigma-Aldrich, St. Louis, MO, USA), hydrochloric acid (37 %, Scharlab, Barcelona, Spain), ethylenediaminetetraacetic acid (EDTA) (Merck, Darmstadt, Germany), sodium fluoride (Panreac AppliChem, Barcelona, Spain), magnesium chloride (Merck, Darmstadt, Germany), protease inhibitor cocktail (*complete Ultra Tablets, Mini, EDTA-free, EASYpack*) (Roche, Basel, Switzerland) and protease type XIV from *Streptomyces griseus* (Sigma-Aldrich, St. Louis, MO, USA) were used to prepare buffers for cell lysis and enzymatic hydrolysis of protein extracts. Ammonium hydrogen carbonate and citric acid (Sigma-Aldrich, St. Louis, MO, USA), ammonia (33 %, Panreac AppliChem, Barcelona, Spain) and methanol (Scharlab, Barcelona, Spain), were employed for the preparation of chromatographic mobile phases. For ICP-MS analysis, 1000 mg L^{-1} standard solutions of Se, Pt, Y, Ir (Merck, Darmstadt, Germany) were used. For cell culture, Dulbecco's Modified Eagle's Medium (DMEM), fetal bovine serum (FBS), antibiotics (penicillin–streptomycin solution, 100 units/mL), phosphate buffered saline (PBS) and trypsin/EDTA solution (0.25 %:0.1 %) were acquired from Gibco (Life Technologies, Thermo Fisher Scientific, Waltham, MA, USA). Trypan Blue solution (Sigma-Aldrich, St. Louis, MO, USA) was used for cell staining, while MTT (3-[4,5-dimethylthiazol-2-yl]-2,5 diphenyl tetrazolium bromide) (Sigma-Aldrich, St. Louis, MO, USA) and dimethyl sulfoxide (DMSO) (Scharlab, Barcelona, Spain) were employed for MTT assays.

2.2. Synthesis and characterization of Ch-SeNPs

Synthesis of Ch-SeNPs was carried out according to a modified version of the method described by Bai et al. [17]. Briefly, 10 mL of an aqueous solution of 0.5 % (m/v) chitosan, previously filtered with a nylon syringe filter with a diameter of 0.45 μm, were mixed with 4.93 mL of 0.35 M ascorbic acid and 5 mL of 0.96 M acetic acid, with magnetic stirring. Then, 1.35 mL of 0.1 M sodium selenite were slowly added, drop by drop, to the mixture. Colour changed instantly to strong red due to a fast formation of colloidal selenium. The solution was completed to a final volume of 45 mL with water, and 5 min later the stirring was stopped. Finally, synthetized Ch-SeNPs were dialysed against 1.5 L of Milli-Q water for 3 h, changing the dialysis medium for fresh water after every hour. The dialysis tubing cellulose membranes employed, with a MWCO of 14 kDa and an inner diameter of 25 mm, were acquired from Sigma-Aldrich (St. Louis, MO, USA). Dialysed Ch-SeNPs solution was stored at 4 °C. Se content in the synthesised SeNPs was quantified following the same procedure for sample acid digestion and ICP-MS analysis as described in **Section 2.6**.

Ch-SeNPs were characterised by TEM-EDS (Transmission Electron Microscopy-Energy Dispersive X-ray Spectroscopy) analysis using a *JEM 2100* microscope (JEOL, Tokyo, Japan). SeNPs solutions were sonicated for 10 min in an ultrasonic bath to favour deagglomeration of particles, prior to their deposition onto copper grids covered with a holey carbon film. Then, Ch-SeNPs were analysed at 200 kV to obtain information about their morphology, size and chemical composition. Size distribution histograms for Ch-SeNPs were constructed after measuring diameters for more than 100 different nanoparticles, employing the image processing program ImageJ (https://imagej.nih.gov/ij/).

2.3. Cell cultures and exposure to cisplatin, SeMet and Ch-SeNPs

HeLa and RPTEC/TERT1 cell lines were obtained from ATCC (Manassas, VA, USA) and Evercyte (Vienna, Austria), respectively. RPTEC/TERT1 were grown in ProxUp medium (Evercyte), while HeLa required DMEM medium supplemented with 10 % (v/v) FBS. In both cases, a mixture of antibiotics (penicillin–streptomycin solution, 100 units/mL) was added to the culture medium. After cell seeding in P100 Petri dishes (Corning Inc., Corning, NY, USA), cultures were maintained in a CO_2 incubator (Thermo Fisher Scientific, Waltham, MA, USA), at 37 °C and 5 % CO_2. Exposure to cisplatin, SeMet, Ch-SeNPs and sodium selenite was done once a cell confluence higher than 70 % was achieved. In the case of the Pt-based drug, it was dissolved in 0.9 % NaCl solution prior to its use, as it was also done for SeMet and sodium selenite. The dispersion with Ch-SeNPs was sonicated for 10 min using an *Elmasonic S60* ultrasonic bath (Elma, Singen am Hohentwiel, Germany) before their addition to the culture media. Finally, cell plates were independently exposed to cisplatin, SeMet, Ch-SeNPs and sodium selenite, or co-incubated with the Pt-drug and either SeMet or Ch-SeNPs, at concentrations of 9 mg L^{-1} for cisplatin and 5 mg L^{-1} for each selenocompound (referred as elemental Se). Control samples were also prepared for comparative purposes. Incubations were maintained for 24 and 48 h. To monitor and photograph cell evolution, an *AE31 Elite* inverted microscope equipped with a *Moticam 3000* camera (Motic, Hong Kong, China) was employed.

2.4. Determination of cell viability by MTT assays

To quantify the degree of cytotoxicity after treatments with cisplatin and the selenocompounds, MTT (3-[4,5-dimethylthiazol-2-yl]-2,5 diphenyl tetrazolium bromide) assays both for HeLa and RPTEC/TERT1 were done. Firstly, 50,000 cells per well were seeded in flat bottom 96-well plates (Thermo Fisher Scientific, Waltham, MA, USA). After 24 h, cells were exposed to the agents at the concentrations indicated in **Section 2.3**, for 24 and 48 h (200 μL/well). Five replicates were prepared for each experiment. Finally, 50 μL of a solution containing 2 mg

mL^{-1} MTT in PBS were added in each well. Plates were incubated for 4 h at 37 °C. Finally, culture media were discarded and DMSO was added (100 μL per well) to dissolve formazan crystals, and the absorbance at 595 nm of each sample was determined after 15 min incubation with a *Sunrise* microplate reader from Tecan (Männedorf, Zurich, Switzerland). Cell viability results (%) were obtained from the ratio between absorbance values of control and exposed cells.

2.5. Microscopy study of cell ultrastructure

Changes in the cell ultrastructure of HeLa and RPTEC/TERT1 after the 24-hour treatments described in Section 2.3 were assessed by TEM-EDS analysis. Culture media were discarded and attached cells were washed three times with PBS, prior to cell harvesting through trypsinization, and cell pellets were recovered by centrifugation at 230 × g, 4 °C with a *5804 R* centrifuge (Eppendorf, Hamburg, Germany). The cell pellet was resuspended in a fixing solution (1 mL) containing glutaraldehyde (2.5 %, v/v) and p-formaldehyde (4 %, v/v) in PBS, and incubated at 4 °C for 4 h. Once fixed, cells were centrifuged at 230 × g, 4 °C with a *5415 R* microcentrifuge (Eppendorf, Hamburg, Germany), washed three times with PBS, and stored in the same buffer at 4 °C overnight. The next step was an incubation with osmium tetroxide (1 %, v/v) for 1 h at room temperature in the dark, followed by three washes with Milli-Q water. Progressive dehydration of cells was achieved by successive 15-min incubations with acetone:water solutions with increasing proportion of acetone (Scharlab, Barcelona, Spain), from 30 to 100 % (v/v). After this, cells were incubated similarly with Spurr resin:acetone mixtures with increasing proportion of resin between 25 and 100 % (v/v). Finally, cells were resuspended and incubated in pure resin at 70 °C for 48 h, in open tubes. The resulting resin-embedded cells were cut into ultrafine slices with an ultramicrotome, stained with uranyl acetate and chrome citrate, and placed onto copper grids before their TEM-EDS analysis with a *JEM 1400* microscope (JEOL, Tokyo, Japan).

2.6. Determination of intracellular Se and Pt content by inductively-coupled plasma mass spectrometry (ICP-MS)

Se and Pt intracellular contents were determined in HeLa and RPTEC/TERT1 cells exposed to cisplatin and/or SeMet or Ch-SeNPs for 24 or 48 h (three replicates for each case), as indicated in Section 2.3. Cells were washed three times with PBS and incubated 5 min with 0.25 % trypsin/0.1 % EDTA solution to detach cells. 10 μL of the resulting cell suspension were mixed with 10 μL of Trypan blue solution and measured with a *Countess II* automated cell counter (Invitrogen, Thermo Fisher Scientific, Waltham, MA, USA) to estimate the number of cells in each culture ($> 5 \times 10^6$ in all cases). After centrifugation, supernatant was discarded and the pellet was washed with PBS.

Cell pellets were microwave-digested with a 3:1 (v/v) mixture containing 65 % HNO_3 and 33 % H_2O_2, using a *MARS* microwave digestion oven equipped with *Xpress* PTFE vessels (CEM Corporation, Matthews, NC, USA). The program applied was: initial 20-min ramp temperature until 130 °C, 15-min heating at 130 °C, and final progressive cooling. Before their direct nebulization analysis by ICP-MS, digested samples were diluted with water to decrease the content of HNO_3 below 2 % (v/v). A quadrupole *Agilent 7700x* ICP-MS (Agilent Technologies, Santa Clara, CA, USA) was used using the operating conditions listed in Table 1. To quantify Se and Pt in samples, external calibration with aqueous standards was employed, in the range of 0.5–200 μg L^{-1} for Se and 0.05–20 μg L^{-1} for Pt. Y (1 μg L^{-1}) and Ir (1 μg L^{-1}) were also added as internal standards, respectively, for matrix effect correction. Results were calculated as the mass of Se or Pt (fg) per cell.

2.7. Determination of Pt bound to nuclear DNA by ICP-MS

Nuclear DNA was extracted and purified from cell pellets obtained as described in Section 2.3, employing a *PureLink™ Genomic DNA Mini Kit* from Invitrogen (Thermo Fisher Scientific, Waltham, MA, USA), following the manufacturer's manual. Cells were resuspended in PBS, lysed with Proteinase K, and incubated with RNAse A to degrade residual RNA. The DNA-containing lysate was mixed with ethanol and a binding buffer, and then purified with a silica-based spin microcolumn with selective binding to DNA. Once washed with two different washing buffers, DNA was finally eluted using 100 μL of the elution buffer. Then, purity and concentration of isolated DNA were measured with a *NanoDrop One* microvolume UV–Vis spectrophotometer (Thermo Fisher Scientific, Waltham, MA, USA). The content of DNA-bound Pt was determined through ICP-MS analysis, as described in Section 2.6. Results were calculated as the mass of Pt per mass of DNA (μg g^{-1}).

Table 1
Instrumental parameters employed for ICP-MS, SEC and AEC analysis.

ICP-MS settings (Agilent 7700x)	
RF Power	1300 W
Plasma gas flow rate	12 mL min^{-1} (Ar)
Auxiliary gas flow rate	1 mL min^{-1} (Ar)
Carrier gas flow rate	1 mL min^{-1} (Ar)
Peristaltic pump rate	0.1 rps (for direct nebulization analysis)
Nebulizer	Conikal (Meinhard)
Spray chamber	Scott
Acquisition mode	- Spectrum (for direct nebulization analysis) - Time resolved analysis (TRA) (for chromatography)
Isotopes monitored	- Analytes: Se (76, 77, 78, 82), Pt (194, 195) - Internal standards: Y (89), Ir (191, 193) (only for direct nebulization analysis)
Dwell time	100 ms
SEC (Size Exclusion Chromatography) conditions	
Chromatographic column	Superdex 75 10/300 GL SEC column (3–70 kDa) (300 x 10 mm id, 13 μm particle size)
Mobile phase	50 mM ammonium hydrogen carbonate (pH 8.4)
Elution mode	Isocratic
Flow rate	0.8 mL min^{-1}
Injection volume	100 μL (SEC-ICP-MS) or 20 μL (SEC-UV/Vis)
Wavelenght for absorbance	280 nm (only for SEC-UV/Vis)
AEC (Anion Exchange Chromatography) conditions	
Chromatographic column	Hamilton PRP-X100 Anion Exchange HPLC column (250 x 4.1 mm id, 10 μm particle size)
Mobile phase	10 mM ammonium citrate, 2 % methanol (pH 5.0)
Elution mode	Isocratic
Flow rate	1 mL min^{-1}
Injection volume	100 μL

2.8. Speciation study of cytosolic Se and Pt by liquid chromatography (LC) coupled to ICP-MS and UV/Vis

2.8.1. Extraction of cytosolic fraction from cells and analysis by size exclusion chromatography (SEC) coupled to ICP-MS or UV/Vis

Cytosolic fractions were obtained from cell pellets of 24-hour cultures prepared as observed in Section 2.3. Cell pellets were washed and lysed with 100 μL of a buffer containing 1 % Triton X-100, 0.5 M NaCl, 20 mM Tris-HCl (pH 8.0), 10 mM EDTA, 50 mM NaF, 5 mM $MgCl_2$ and a protease inhibitor cocktail (one tablet per 10 mL of buffer). Subsequently, lysates were kept in ice, sonicated with a *Vibra-Cell™ VCX 130* ultrasound probe (Sonics & Materials Newtown, CT, USA), applying 20 pulses/sample (2 s "on" and 5 s "off") and 40 % of amplitude. Samples were incubated for 15 min in a *Thermomixer compact* shaker (Eppendorf, Hamburg, Germany) at 4 °C and ultracentrifuged (13,000 rpm, 4 °C, 10 min). The supernatant, where most cytosolic proteins are present, was kept at −20 °C until analysis.

Extracts were analysed by SEC-ICP-MS or SEC-UV/Vis, to register

both cytosolic biomolecules containing Se and Pt and protein profile. Aqueous solutions of cisplatin and various Se species (selenite, selenate, $(SeCys)_2$, MeSeCys, SeMet and Ch-SeNPs) were also measured for comparative purposes. Samples were injected directly for SEC-ICP-MS analysis whereas a previous 1:4 dilution with mobile phase was done in the case of SEC-UV/Vis.

Chromatographic separation was achieved with a *Superdex 75 10/300 GL* SEC column (3–70 kDa) from Amersham Biosciences (GE Healthcare, Little Chalfont, Buckinghamshire, UK) and a delivery system consisting on a *PU-2089 Plus* HPLC pump (Jasco, Tokyo, Japan), equipped with an injection valve (Rheodyne, IDEX Health & Science, Rohnert Park, CA, USA) and a 20 μL or 100 μL sample loop for SEC-UV/Vis and SEC-ICP-MS, respectively. In the first case, the detection was carried out with a *MD-2018* UV/Vis spectrophotometer (Jasco, Tokyo, Japan) at a wavelength of 280 nm. Table 1 shows the main conditions and instrumental parameters used for SEC-UV/Vis and SEC-ICP-MS analysis. Calibration of the chromatographic column was also done by SEC-UV/Vis measurements of a series of proteins and peptides with different molecular weights acquired from Sigma-Aldrich (St. Louis, MO, USA): transferrin (79.5 kDa), bovine serum albumin (66 kDa), carbonic anhydrase (29 kDa), myoglobin (16.7 kDa), cytochrome *c* (12.4 kDa), aprotinin (6.5 kDa) and coenzyme B12 (1.55 kDa).

2.8.2. Enzymatic hydrolysis of cytosolic extracts and Se speciation analysis by anion exchange chromatography (AEC) coupled to ICP-MS

Cytosolic fractions were obtained from cell pellets as described in **Section 2.8.1** without including protease inhibitors in the buffer. Extracts were mixed 1:1 with a pH 7.0 solution of 800 mg L^{-1} protease type XIV from *Streptomyces griseus* in a *TAE* buffer containing 40 mM Tris, 20 mM acetic acid and 1 mM EDTA, measuring the resulting pH with a pH-meter *BASIC 20* (Crison Instruments, Barcelona, Spain). The samples were incubated at 37 °C for 24 h, with continuous agitation (300 rpm) in a *Thermomixer compact* shaker (Eppendorf, Hamburg, Germany). For AEC-ICP-MS measurements, hydrolysed extracts were injected without dilution into a *PRP-X100* column equipped with a column guard (Hamilton, Reno, NV, USA). The instrumental parameters used are indicated in Table 1. To identify Se species, standard aqueous solutions of selenite, selenate, $SeCys_2$, MeSeCys, SeMet, oxidised SeMet (SeOMet) and SeNPs were analysed in parallel. Species confirmation was performed by spiking the extracts with the standard Se-compounds. SeOMet was obtained by mixing an aqueous solution of SeMet 1:4 (v/v) with H_2O_2 followed by 40 min shaking.

2.9. Statistical analysis

Statistical analysis was applied to the cell viability and the intracellular Pt and Se data, where all the measurements were performed in quintuplicate and the results expressed as the mean value ± the standard deviation. One-way analyses of variance (ANOVA) and two tailed t-tests with 95 % of confidence level were performed, employing the Analysis ToolPak of Microsoft Excel Professional Plus 2019 software.

3. Results and discussion

3.1. Characterization of synthesized Ch-SeNPs

TEM-EDS analysis of the dispersion obtained after the Ch-SeNPs synthesis described in **Section 2.2** showed the presence of Se in the form of spherical and non-agglomerated particles, with an average diameter close to 40 nm (Fig. 1), which is in the size range of most of the nanoparticles found in the literature with efficient cellular uptake [18]. Ch-SeNPs remained disaggregated at least one month after their synthesis. Furthermore, no changes were observed in their sphericity, size and aggregation degree after being added to the culture media employed for cell experiments (data not shown), confirming the stabilising effect of the polysaccharide chitosan [15,19]. ICP-MS analysis of the SeNPs suspension provided a concentration of 195 ± 10 mg Se L^{-1} (n = 5).

3.2. Cell viability assays to evaluate the nephroprotective potential of SeMet and Ch-SeNPs against cisplatin

RPTEC/TERT1 and HeLa were employed as models of renal and cancer cells, respectively, with the aim to evaluate the potential nephroprotective effect of SeMet and Ch-SeNPs while maintaining the antitumour activity of cisplatin.

First, the biocompatibility of SeMet and Ch-SeNPs was evaluated in the absence of the Pt-drug, and compared with selenite (Se(IV)) as a reference compound with well-known antioxidant and antitumour effect [20]. A Se concentration of 5 mg L^{-1} was used in all cases, incubating cells at 24 and 48 h. Cell viability results from MTT assays and microscope images of the corresponding cultures can be seen in Figs. 2-4, respectively. No relevant damage was found in RPTEC/TERT1 after SeMet or Ch-SeNPs exposure up to 48 h, neither in the percentage of viable cells (Fig. 2**a**) nor in their appearance (Fig. 3**a-c**). On the contrary, although SeMet does not cause a relevant effect in HeLa cells, some decrease in viability after the first 24 h of incubation with Ch-SeNPs was

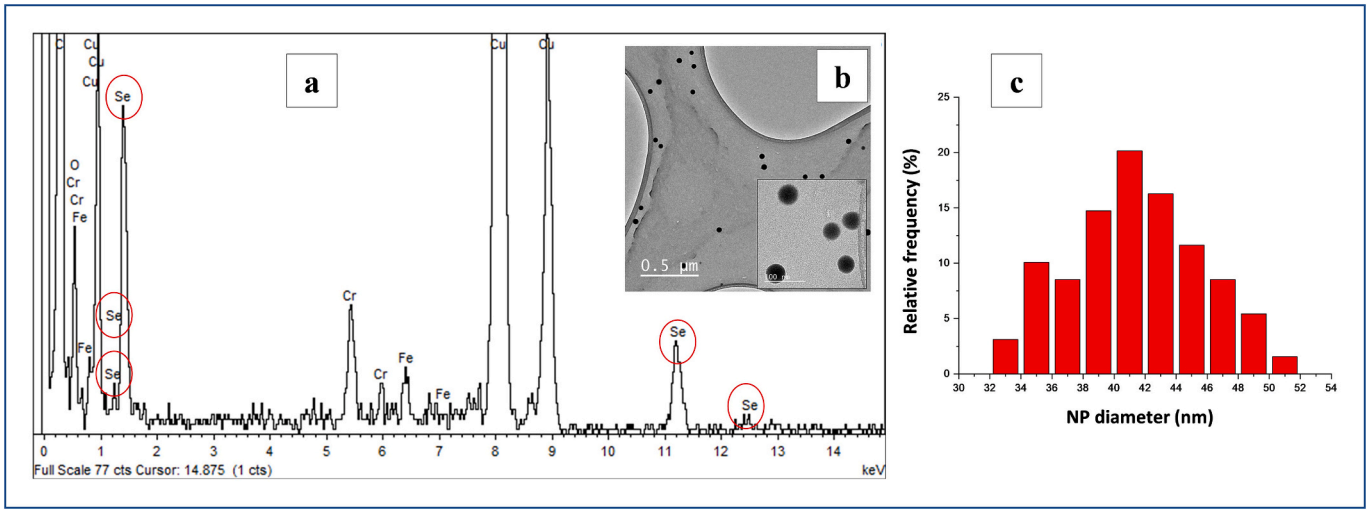

Fig. 1. Results obtained from TEM-EDS analysis of synthetised Ch-SeNPs: EDS spectra with the elemental composition of the particles (a); TEM images showing size, morphology and aggregation degree of the particles (b); histograms of particle diameter distribution constructed after measuring the size of more than 100 nanoparticles (c).

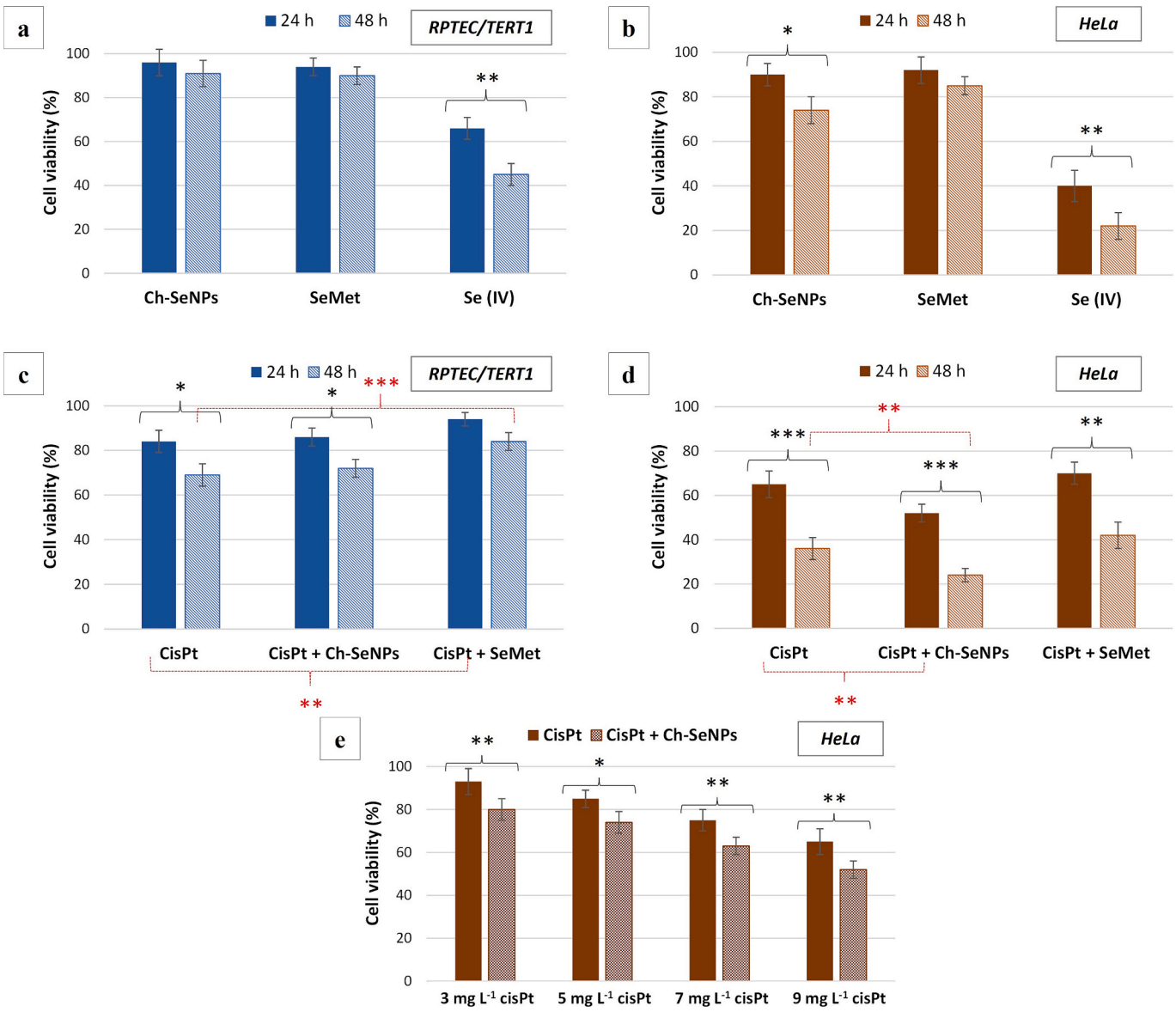

Fig. 2. Cell viability results from MTT assays of 24 and/or 48-hour cultures of RPTEC/TERT1 (a, c) and HeLa (b, d, e): after exposure to Ch-SeNPs, SeMet or sodium selenite (5 mg L^{-1} in all cases, expressed as Se concentration) (a, b); after exposure to cisplatin (cisPt) (9 mg L^{-1}) alone or combined with Ch-SeNPs or SeMet (5 mg L^{-1} of Se in both cases) (c, d); after 24-hour exposure to different concentrations of cisplatin (3, 5, 7 or 9 mg L^{-1}) alone or combined with Ch-SeNPs (5 mg L^{-1}) (e). Values are represented as the average ± the standard deviation (n = 5). Statistically significant differences were considered when p-value was lower than 0.05: $p < 0.05$ (*), $p < 0.01$ (**) and $p < 0.005$ (***).

observed (Fig. 2**b**), in accordance with the expected anticancer potential of SeNPs [14–16].

Thereby, these particles may selectively attack tumour cells as reported in previous works where not only the antineoplastic potential of SeNPs but also their effect over renal cell lines such as HK-2 and HEK-293 was evaluated [21–23]. The higher secretion of acid compounds due to the altered metabolic activity of cancer cells [24] could be an important factor in this regard, as it would favour the pro-oxidant behaviour of SeNPs, leading to ROS increase and higher cell death rate. In contrast, they would act as antioxidants in healthy cells, showing a beneficial redox duality [13–15]. On the other hand, SeNPs could arrest cell cycle at the S-phase just before mitosis [25], a circumstance that would have more incidence for tumour cells due to their faster proliferation. Regarding the use of selenite, it produced a high degree of cell death in both cell types, being more than 50 % and 75 % for RPTEC/TERT1 and HeLa, respectively, after 48 h of exposure (Fig. 2**a, 2b**). This confirms the lower toxicity and higher biocompatibility of organic selenospecies such as SeMet, as well as SeNPs, compared to inorganic Se (IV) [13–15].

The nephroprotective potential of SeMet and Ch-SeNPs was evaluated by measuring cell viability under exposure to 9 mg L^{-1} cisplatin alone or combined with 5 mg L^{-1} of each of the selenocompounds (expressed as Se content), simultaneously monitoring possible changes in the antitumour efficacy of the Pt-drug. Cisplatin concentration was selected according to previous works, in order to produce a significant mortality which allowed assessing the potential protective effect of the tested compounds [26]. MTT results (Fig. 2**c, 2d**) indicated that the incubation with the Pt-drug caused an increasing cell mortality over time. The damage was especially severe for HeLa, showing a viability lower than 40 % after 48 h, being half the value corresponding to RPTEC/TERT1 at the same incubation time. Cisplatin toxicity was also observed in micrographs (Fig. 3**a-e and** Fig. 4**a-e**), as it provoked an increase in cell detachment, worsen contact between adherent cells and altered their normal shape, being these effects more acute for HeLa.

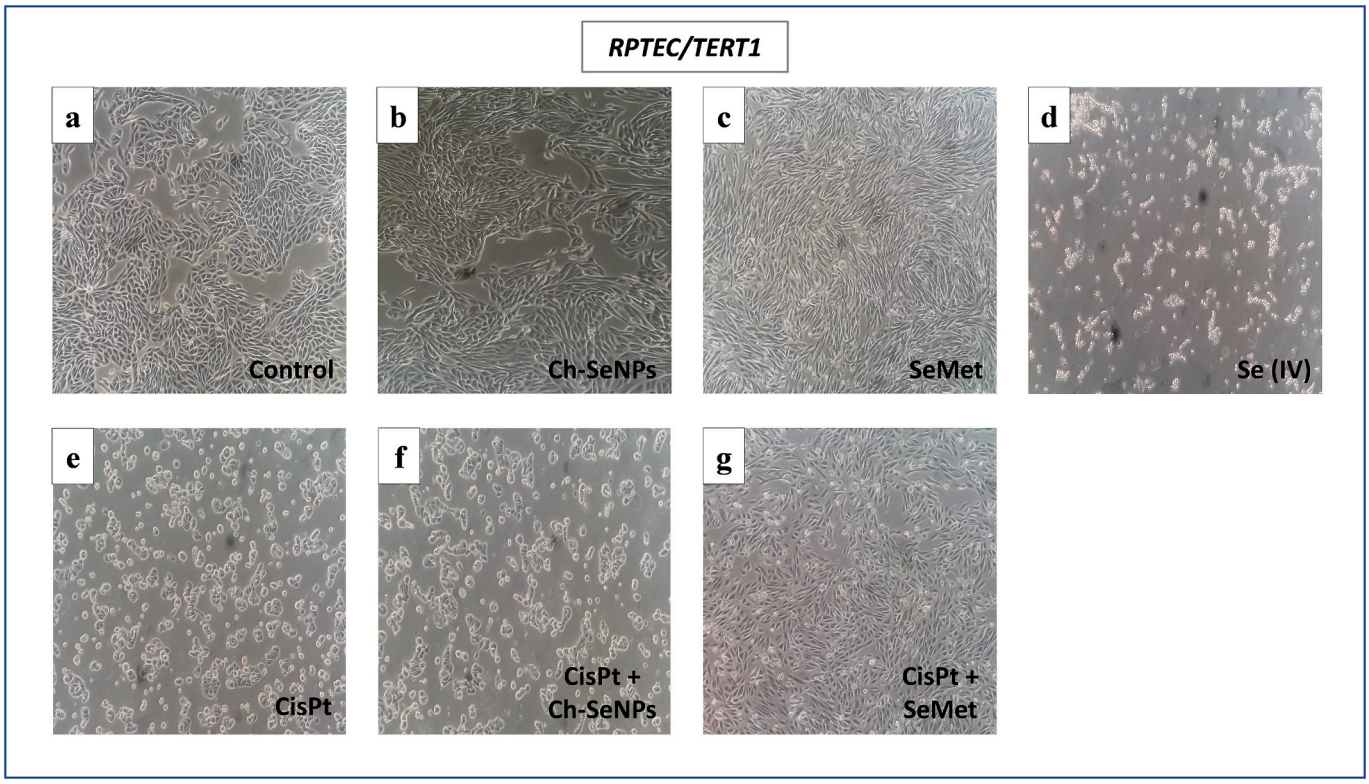

Fig. 3. Inverted microscope images at 10x magnification obtained from 48-hour cultures of RPTEC/TERT1: control cells (a); cells treated with Ch-SeNPs (5 mg L^{-1} of Se) (b); cells treated with SeMet (5 mg L^{-1} of Se) (c); cells treated with sodium selenite (5 mg L^{-1} of Se) (d); cells treated with cisplatin (9 mg L^{-1}) (e); cells treated with cisplatin (9 mg L^{-1}) and Ch-SeNPs (5 mg L^{-1} of Se) (f); and cells treated with cisplatin (9 mg L^{-1}) and SeMet (5 mg L^{-1} of Se) (g).

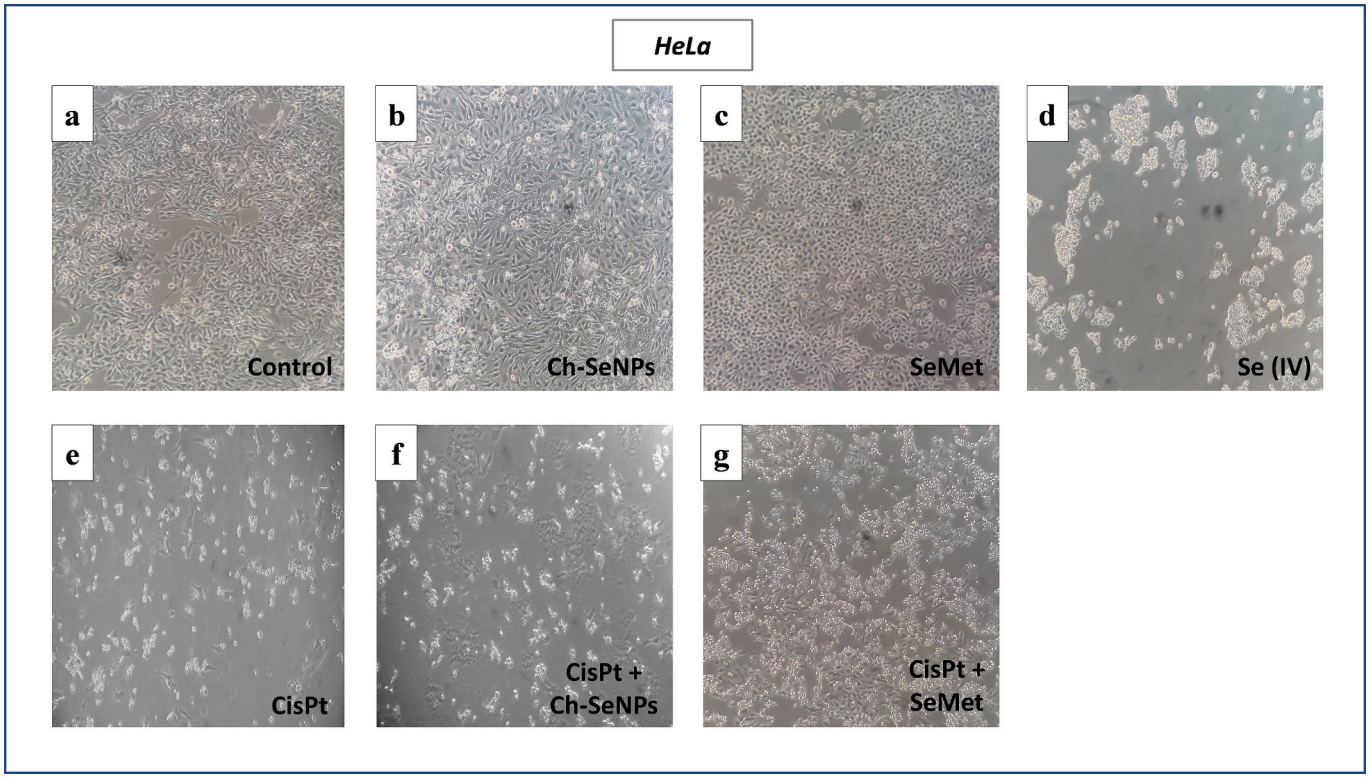

Fig. 4. Inverted microscope images at 10x magnification obtained from 48-hour cultures of HeLa: control cells (a); cells treated with Ch-SeNPs (5 mg L^{-1} of Se) (b); cells treated with SeMet (5 mg L^{-1} of Se) (c); cells treated with sodium selenite (5 mg L^{-1} of Se) (d); cells treated with cisplatin (9 mg L^{-1}) (e); cells treated with cisplatin (9 mg L^{-1}) and Ch-SeNPs (5 mg L^{-1} of Se) (f); and cells treated with cisplatin (9 mg L^{-1}) and SeMet (5 mg L^{-1} of Se) (g).

On the other hand, when cisplatin was combined with SeMet, viability in renal cells increased compared to the cultures with the Pt-drug alone (84 % and 69 % at 48 h, respectively) (Fig. 2**c**). This confirms the protective potential previously reported for SeMet, which may be related to a partial deactivation of cisplatin due to the formation of complexes with SeMet [11,12]. In the case of HeLa cells (Fig. 2**d**), co-administration of cisplatin with SeMet showed no significant effect on the antitumour efficacy of the Pt-drug.

The employment of Ch-SeNPs on cisplatin-treated RPTEC/TERT1 cells produced no significant changes on the viability and morphology

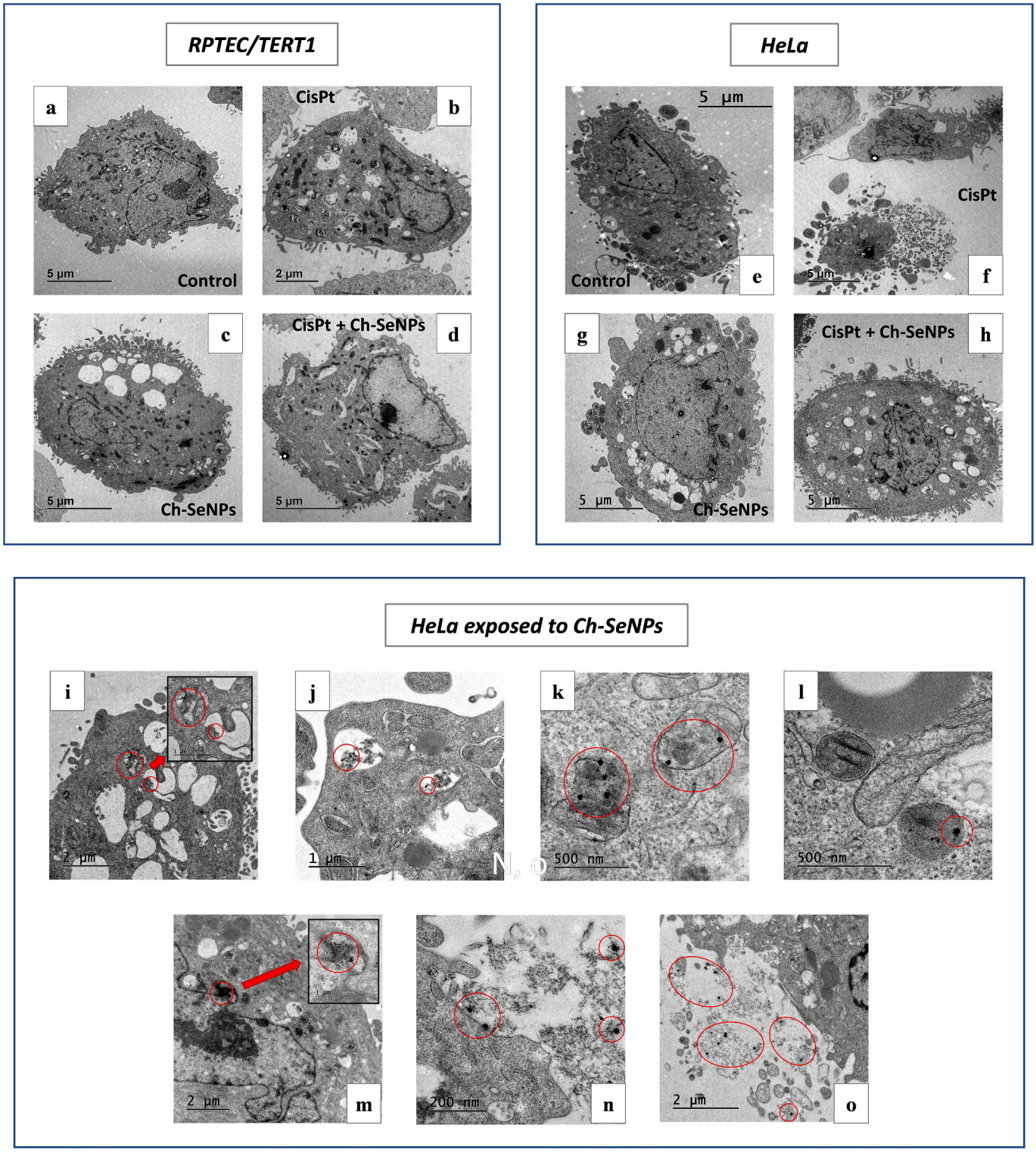

Fig. 5. TEM images of cell ultrastructure obtained from 24-hour cultures of RPTEC/TERT1 (a-d) and HeLa (e-h, i-o): control cells (a, e); cells treated with cisplatin (9 mg L^{-1}) (b, f); cells treated with Ch-SeNPs (5 mg L^{-1}, expressed as Se concentration) (c, g, i-o); cells co-administered with Ch-SeNPs (5 mg L^{-1}) and cisplatin (9 mg L^{-1}) (d, h). Images i-o show different locations (red circles) of Ch-SeNPs after being administered to HeLa cells: vacuoles (i, j); mitochondria (k); lysosomes (l); nucleus (m); plasma membrane, cell fragments and exosomes (n, o). (For interpretation of the references to colour in this figure legend, the reader is referred to the web version of this article.)

shown by cells treated with cisplatin alone (Fig. 2**c and** Fig. 3**e, 3f**). In contrast, a significant increase of HeLa mortality took place when the Pt-drug was co-administered with Ch-SeNPs since the first 24 h of incubation (around 15 %) (Fig. 2**d**), suggesting a synergistic effect between the antineoplastic activity of the two agents. Cell viability was also quantified in HeLa cells exposed for 24 h to different concentrations of the Pt-drug (3–9 mg L^{-1}) alone or in the presence of Ch-SeNPs (5 mg L^{-1}), being always lower in the second case (Fig. 2**e**). For example, taking as reference the cytotoxic effect produced with 9 mg L^{-1} cisplatin (viability of 65 %), this was comparable to that observed with the co-incubation with Ch-SeNPs and 7 mg L^{-1} of the Pt-drug. This represents about 20 % reduction in cisplatin dose for the same antitumour effect. Thus, the concomitant application of both agents could allow lower drug doses without loss of treatment efficacy as well as a decreased risk of kidney impairment.

3.3. Analysis of cell ultrastructure after the exposure to cisplatin and selenocompounds

For a better understanding of the effects of the selenocompounds and cisplatin inside RPTEC/TERT1 or HeLa cells, their morphology and subcellular structure were also studied by TEM-EDS analysis in 24-h cell cultures, as described in **Section 2.5**. The micrographs obtained are shown in Fig. 5. After cisplatin incubation, a significant number of cells presented a slight increase in the amount of endosomal vacuoles compared to control samples, regardless of the cell line considered (Fig. 5**a, 5b 5e, 5f**). This may result from an overstimulated autophagy which could be explained both as a mechanism of resistance or a pro-apoptotic factor [27]. Regarding the plasma membrane integrity, severe damage was observed in different HeLa cells (Fig. 5**f**) with extensive cell fragmentation, as a sign of advanced apoptosis, while RPTEC/TERT1 remained mostly unchanged (Fig. 5**b**). This may be related to the potential of cisplatin to alter the fluidity, permeability and structure of cell membranes through interactions with lipids and proteins [28]. Cells treated with SeMet alone or combined with cisplatin (data not shown) showed no significant vacuolisation or plasma membrane damage, demonstrating its ability to revert the cisplatin-induced autophagy (Fig. 5**a, 5b 5e, 5f**), in agreement with the recovery of cell viability in RPTEC/TERT1 shown in **Section 3.2**.

On the contrary, incubation with Ch-SeNPs had a strong impact on cell ultrastructure, giving rise to the formation of multiple and large cytoplasmic vacuoles both in RPTEC/TERT1 and HeLa (Fig. 5**c, 5g**). Furthermore, the internalization of Ch-SeNPs by both cell lines was observed, reaching different subcellular organelles, such as vacuoles (Fig. 5**i, 5j**), mitochondria (Fig. 5**k**), lysosomes (Fig. 5**l**) and nucleus (Fig. 5**m**). Some Ch-SeNPs were also present within the plasma membrane, cell fragments and exosomes (Fig. 5**n, 5o**). This is in agreement with the endocytosis pathway typically associated with the cellular uptake of SeNPs, transfer to organelles and removal by exocytosis [13,15,16]. It is worth noting the low amount of nanoparticles observed within the cells compared to the number of vacuoles, which were empty in most cases (Fig. 5**i, 5j**). This might suggest that most of the internalised Ch-SeNPs were released from cells after the 24-hour incubation or transformed into ionic Se or other selenospecies, thus not being longer visible by TEM. Besides, not all the vacuoles formed after SeNPs exposure may be involved in their capture and intracellular transport but also in further autophagic or osmotic processes [29,30].

When cells were simultaneously exposed to Ch-SeNPs and cisplatin, less internalized particles were found and the number and size of vacuoles also decreased regardless of the cell line considered (Fig. 5**d, 5h**). No signs of a higher release were observed in terms of Ch-SeNPs present in extracellular fragments, so their lower amount may be result of a decreased uptake related to the alterations in plasma membrane after cisplatin treatment [28]. Although the effect of the Pt-drug on the internalization of SeNPs has not been described yet, it could have some similarities with other known mechanisms altered by this compound. Cisplatin is able to impair the receptor-mediated endocytosis of proteins through inhibition of vacuolar H^+-ATPase [31], thus it could be thought to decrease as well the internalization of SeNPs since this process may be limited by inhibiting ATP synthase [15]. Nevertheless, the activity of internalised Ch-SeNPs was still noticeable, as death rate in HeLa increased when both agents were added to the cultures (**Section 3.2**).

3.4. Determination of Se and Pt intracellular content

Se and Pt internalisation was evaluated by ICP-MS analysis in RPTEC/TERT1 and HeLa cells after 24 and 48-h exposure to SeMet, Ch-SeNPs and their co-administration with cisplatin (Fig. 6). The exposure to both selenocompounds increased the intracellular content of Se (Fig. 6**a, 6b**) compared to control samples in both cell lines. These results are in agreement with those previously reported for HeLa, A375 and K562 cancerous cell lines incubated with SeNPs or SeMet [21,32]. Se content was almost double for cells exposed to Ch-SeNPs compared to SeMet, despite the fact that SeMet is considered one of the selenospecies with higher cellular internalisation [32].

HeLa was the cell line with the lowest Se uptake after 24 h (130 fg Se $cell^{-1}$ for Ch-SeNPs, and 65 fg Se $cell^{-1}$ for SeMet), being about 50 % of the internalisation found in RPTEC/TERT1 regardless of the selenocompound employed (Fig. 6**a, 6b**), which may be related to less efficient endocytic mechanisms in the tumour cells.

The co-administration of cisplatin with both selenocompounds led to a significant reduction in Se uptake (Fig. 6**a, 6b**), especially for HeLa. RPTEC/TERT1 internalised 12 % and 48 % less Se in 24-hour cultures with Ch-SeNPs and SeMet, respectively, whereas Se levels decayed 62 % and 46 % for cancer cells, with a higher decrease after 48 h. This might be explained by a deleterious effect caused by the Pt-drug on cellular mechanisms involved in the internalisation of Se compounds, as suggested in **Section 3.3**, and the formation of complexes between SeMet and cisplatin and their further excretion [12]. Despite this reduced uptake, both Ch-SeNPs and SeMet are able to exert a pharmacological action over cells, in agreement with cell viability assays described in **Section 3.2**.

Regarding Pt analysis, higher intracellular content was found for RPTEC/TERT1 compared to HeLa cells (Fig. 6**c, 6d**). When cisplatin was supplied alone, kidney cells presented a similar Pt level after 24 and 48 h (59 and 54 fg Pt $cell^{-1}$, respectively), while it dropped more than 50 % for HeLa (from 46 to 21 fg Pt $cell^{-1}$). Hence, saturation uptake may be achieved during the first 24 h in both cell lines, although a significant reduction in Pt content occurred for HeLa after that time.

Moreover, Pt was also determined in nuclear DNA, the main target of cisplatin, showing values almost 20 % higher in HeLa (Fig. 6**e, 6f**), in consonance with their worse ability to repair damaged DNA. No significant differences were observed between cultures of 24 and 48 h, thus the formation of Pt-DNA adducts seems to reach its maximum in the first day of incubation, with no evidence of DNA recovery after 48 h. This is in agreement with the evolution shown for the total Pt content in RPTEC/TERT1 but not in HeLa, where the accumulation of cisplatin strongly decreased after 48 h (Fig. 6**d**). This may be explained by the less efficient mechanisms for DNA repair in cisplatin-sensitive cancer cells [33], which would have higher dependence on alternative resistance mechanisms such as the modulation of membrane transporters to decrease drug accumulation. In fact, resistant tumour cells have been demonstrated to internalise the Pt-drug to a lesser extent than the parental ones [34,35], and they are also able to enhance its efflux [36]. Although HeLa cells showed reduced Pt cellular uptake, their survival rates were lower than RPTEC/TERT1 (**Section 3.2**), thus confirming the higher impact of the amount of Pt-DNA adducts on the pharmacological effect rather than the total intracellular content of the drug [4].

The values of intracellular Pt after the simultaneous treatment with Ch-SeNPs did not significantly change regardless of the cell line (Fig. 6**c, 6d**). The same was found during the measurement of Pt bound to DNA (Fig. 6**e, 6f**), demonstrating that the presence of SeNPs had no influence

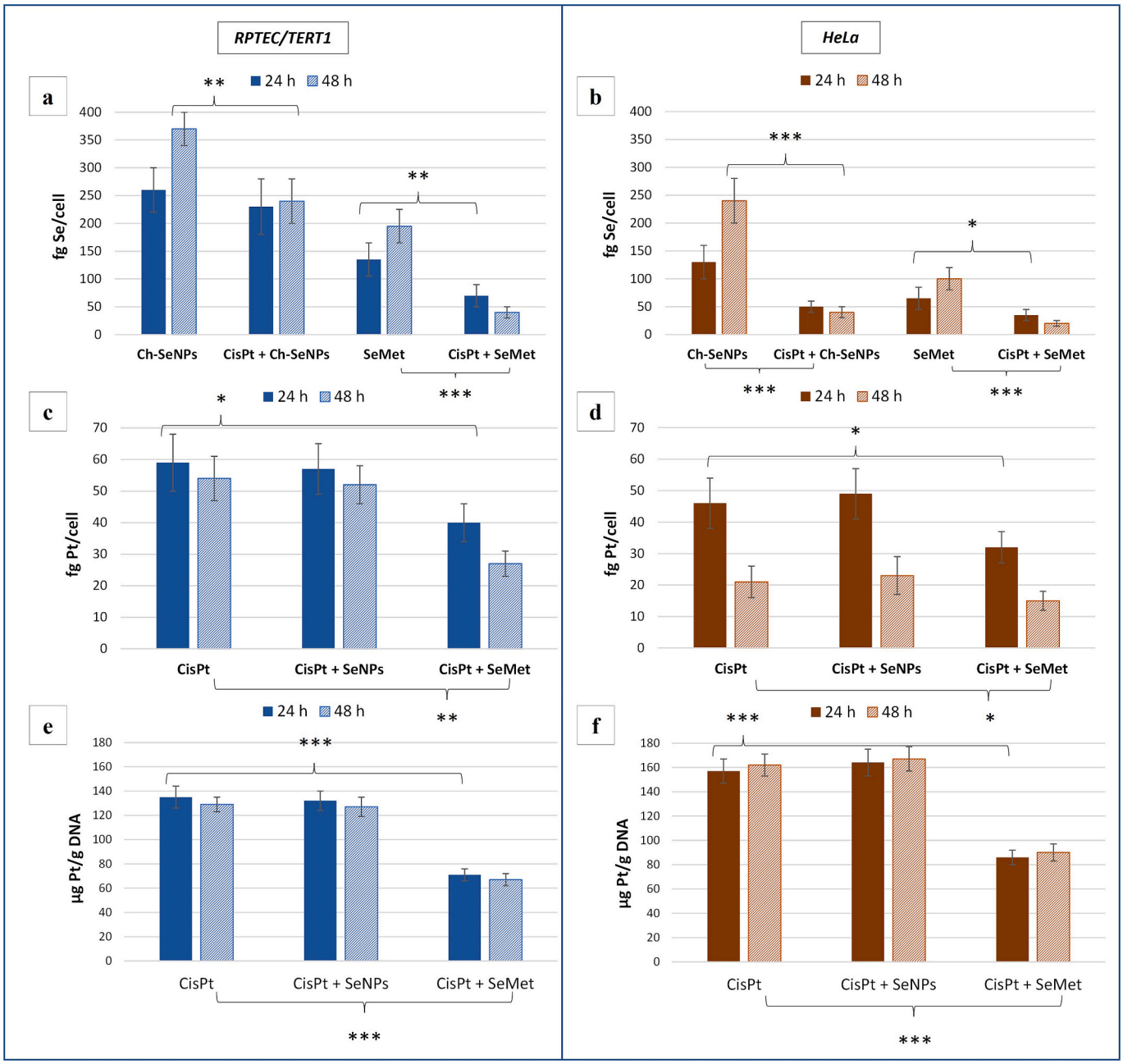

Fig. 6. Values of Se and Pt determined by ICP-MS in 24- and 48-h cultures of RPTEC/TERT1 (a, c, e) and HeLa (b, d, f): intracellular total content of Se (fg Se/cell) after exposure to Ch-SeNPs (5 mg L^{-1} of Se) or SeMet (5 mg L^{-1} of Se) alone or combined with cisplatin (cisPt) (9 mg L^{-1}) (a, b); intracellular total content of Pt (fg Pt/cell) after exposure to cisplatin (9 mg L^{-1}) alone or combined with Ch-SeNPs or SeMet (5 mg L^{-1} of Se in both cases) (c, d); content of Pt-bound to nuclear DNA after exposure to cisplatin (9 mg L^{-1}) alone or combined with Ch-SeNPs or SeMet (5 mg L^{-1} of Se in both cases) (e, f). Control cells presented contents of Se and Pt lower than the LOD (26 fg Se/cell and 0.2 fg Pt/cell), as it also occurred with Se content in cells treated only with cisplatin and with Pt content in cells treated only with selenocompounds. Values are represented as the average ± the standard deviation (n = 3). Statistically significant differences were considered when p-value was lower than 0.05: $p < 0.05$ (*), $p < 0.01$ (**) and $p < 0.005$ (***).

on the internalisation of cisplatin and its further binding to DNA, a critical aspect to preserve its anticancer action. Conversely, the co-administration of SeMet in the first 24 h induced a clear decrease in cisplatin uptake (near 30 %) and Pt-DNA binding (near 45 %) in both cell lines (Fig. 6**c-f**). The total content of intracellular Pt continued decreasing after 48 h in the presence of SeMet (Fig. 6**c, 6d**), but the amount of Pt bound to DNA remained almost the same after 24 and 48 h (Fig. 6**e, 6f**). Thus, SeMet promotes a lower accumulation of the Pt-drug inside cells which also leads to a lower platination degree in DNA. This is in agreement with the findings of García-Sar et al. [12], which reported lower levels of Pt in the kidneys of rats co-treated with cisplatin and SeMet, as well as a reduced number of Pt-DNA adducts. They also observed an increase in the Pt excreted into urine and the presence of Pt-SeMet complexes, which could act as drug scavengers to prevent its cellular accumulation. Thereby, the direct interaction between cisplatin and SeMet (Pt-Se) seems to be the main cause of the nephroprotective effect of this selenoamino acid.

3.5. *Chromatographic analysis of Se and Pt in cytosolic extracts*

Finally, speciation analysis of Se and Pt in cytosolic extracts from 24-hour cell cultures was carried out by LC-ICP-MS, both using SEC and

AEC, including additional UV/Vis detection in the first case.

SEC chromatograms monitoring either absorbance at 280 nm or ^{78}Se or ^{195}Pt signals are displayed in Fig. 7 for RPTEC/TERT1 cell extracts. Chromatograms for renal cells co-treated with cisplatin and Ch-SeNPs show two main peaks of Se and Pt, eluting at minutes 8 (peak A) and 20 (peak B) (Fig. 7**b, 7c**) presenting the highest absorbance at 280 nm (Fig. 7**a**). This confirms that most of cytosolic Se is part of proteins, whereas Pt is mainly bound to them. Regarding Se signals in the SEC chromatograms (Fig. 7**d-i**), these were higher in samples exposed to Ch-SeNPs or SeMet compared to controls. The strongest increase was in peak A (corresponding to molecular weights of 66–79.5 kDa), suggesting a greater presence of high molecular weight selenoproteins due to the effect of both selenocompounds. This is in accordance with the upregulation of activity and expression levels of different selenoproteins reported in cell cultures and animal models after treatment with selenospecies [37–41]. Among them, selenoproteins with molecular weights higher than 60 kDa, such as selenoproteins I, N, O and P, and thioredoxin reductases 1, 2 and 3, would match the molecular weights expected for peak A. This would confirm an overexpression of large selenoproteins in RPTEC/TERT1 induced by both Ch-SeNPs and SeMet. Comparing Se chromatograms, Ch-SeNPs (Fig. 7**e**) seem to enhance selenoprotein synthesis to a greater extent than SeMet (Fig. 7**f**). Co-incubation with cisplatin involved a significant reduction in the intensity of Se peaks for both selenocompounds, in consonance with the decreased Se accumulation observed (**Section 3.4**).

Changes in the SEC profile of cytosolic Pt were also found when comparing extracts from renal cells treated with cisplatin alone or combined with selenocompounds (Fig. 7**j-l**). In the first case, the relative intensity of peak A was clearly lower than that corresponding to peak B (Fig. 7**j**). When SeMet was added, all Pt signals decayed (Fig. 7**l**), as observed for Pt cytosolic levels (**Section 3.4**), but more similar relative intensities between the two peaks were visible compared to those observed when the Pt-drug alone was administered (Fig. 7**j**). On the other hand, after cell incubation with cisplatin and SeNPs, peak A significantly increased (Fig. 7**k**). Therefore, the internalisation of both selenocompounds seems to lead to a redistribution of cytosolic Pt with preferent platination of biomolecules eluting at lower retention times, especially with Ch-SeNPs. This could be related to an increased amount of high-molecular-weight proteins, which would be in agreement with the overexpression of selenoproteins revealed in Se chromatograms (Fig. 7**e-f, 7h-i**).

Pt signal in peak A was much higher when cisplatin was combined with Ch-SeNPs instead of SeMet, whereas the corresponding Se intensity was similar in both samples (Fig. 7**e, 7f, 7k, 7l**). This may be related to the decreased uptake of the Pt-drug after SeMet exposure (**Section 3.4**). Nevertheless, it should be studied if the different Pt intensity in peak A could be also explained by a higher overexpression not only of selenoproteins but also other non-selenium containing proteins larger than 60 kDa in cultures with SeNPs. The higher amount of Pt-binding sites in such proteins would favour a higher platination degree, which could agree with the observed in peak A.

In parallel, Se speciation analysis by AEC-ICP-MS was performed on RPTEC/TERT1 cytosolic fractions previously submitted to an enzymatic hydrolysis (Fig. 8). Control samples showed two main Se peaks around 2 and 3 min, respectively, and a low-intensity peak at 3.5 min, which correspond to $(SeCys)_2$, MeSeCys and Se(IV), respectively (Fig. 8**c**). Peak assignment was done not only by comparison with a mixture of Se standards (Fig. 8**a, 8b**) but also with extracts from control cells doped with each of these compounds after the extraction and further hydrolysis (not shown). No differences were found in cell extracts with cisplatin alone (Fig. 8**d**) compared to controls, so its administration did not seem to alter the selenospecies distribution in cells.

Se chromatograms for cells exposed to either Ch-SeNPs (Fig. 8**e**) or SeMet (Fig. 8**g**) showed differences both in the intensity, profile and ratio of the different Se peaks. In the first case, there was a strong increase in the levels of $(SeCys)_2$ and MeSeCys compared to control samples. MeSeCys was the most abundant species, in accordance with previous studies about the Se metabolism in HepG2 cells incubated with SeNPs [39]. Increased Se(IV) was also observed compared to controls, which could be due to progressive dissolution and oxidation of the SeNPs after entering cell lysosomes [13,15,16]. Considering that cells produce the amino acid SeCys through sequential biotransformations of selenite [42], the increased levels of Se(IV) after SeNPs treatment could be related as well to the higher intensity in the peaks of $(SeCys)_2$ and

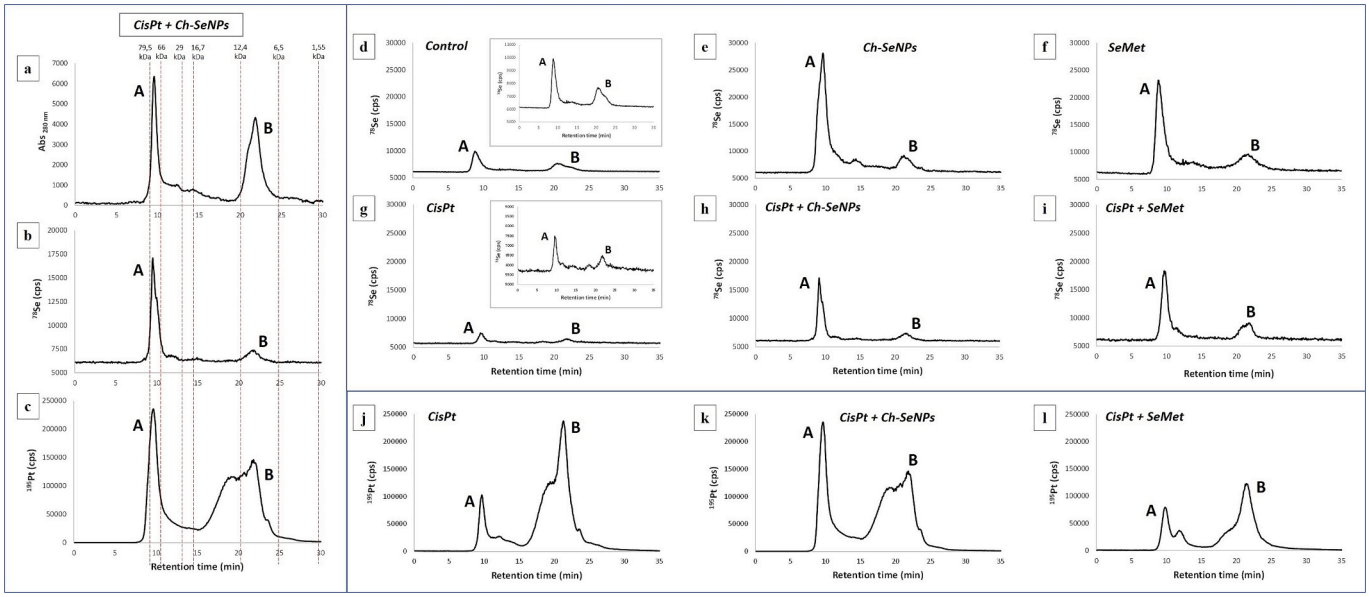

Fig. 7. SEC chromatograms of cytosolic extracts from 24-hour cultures of RPTEC/TERT1. Figures a-c show the chromatograms for extracts from cell cultures with cisplatin (9 mg L^{-1}) and Ch-SeNPs (5 mg L^{-1} as Se): SEC-UV/Vis measurement at 280 nm (a); and SEC-ICP-MS measurements of ^{78}Se (b) and ^{195}Pt (c). Dashed lines represent the molecular weights of different protein and peptide standards. A and B indicate the two peaks with highest intensity in the three cases. ^{78}Se chromatograms by SEC-ICP-MS are shown for control cells (d) and cells exposed to: Ch-SeNPs (5 mg L^{-1} of Se) (e); SeMet (5 mg L^{-1} of Se) (f); cisplatin (9 mg L^{-1}) (g); cisplatin (9 mg L^{-1}) and Ch-SeNPs (5 mg L^{-1} of Se) (h); cisplatin (9 mg L^{-1}) and SeMet (5 mg L^{-1} of Se) (i). ^{195}Pt chromatograms by SEC-ICP-MS are shown for cells exposed to: cisplatin (9 mg L^{-1}) (j); cisplatin (9 mg L^{-1}) and Ch-SeNPs (5 mg L^{-1} of Se) (k); cisplatin (9 mg L^{-1}) and SeMet (5 mg L^{-1} of Se) (l).

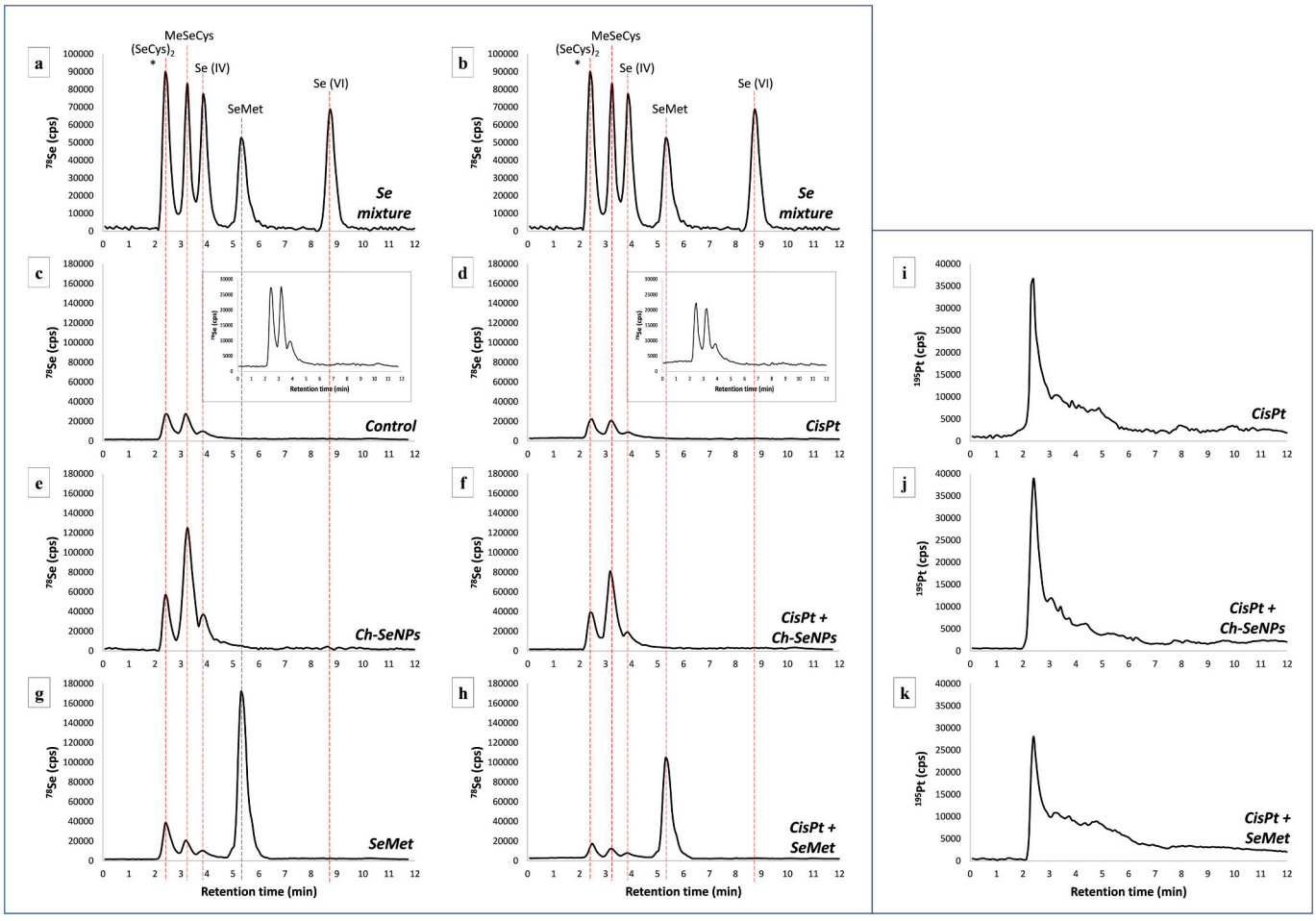

Fig. 8. ^{78}Se and ^{195}Pt chromatograms obtained by AEC-ICP-MS. ^{78}Se chromatograms of a mixture of Se standards ($(SeCys)_2$*, SeMeSeCys, selenite, SeMet, selenate) are shown in a-b as reference to peak assignment. ^{78}Se chromatograms of the hydrolysed cytosolic extracts from 24-hour cultures of RPTEC/TERT1 are shown for control cells (c) and cells exposed to: cisplatin (9 mg L^{-1}) (d); Ch-SeNPs (5 mg L^{-1} of Se) (e); cisplatin (9 mg L^{-1}) and Ch-SeNPs (5 mg L^{-1} of Se) (f); SeMet (5 mg L^{-1} of Se) (g); cisplatin (9 mg L^{-1}) and SeMet (5 mg L^{-1} of Se) (h). *Oxidised SeMet (SeOMet), if present, coelutes with $(SeCys)_2$. ^{195}Pt chromatograms for the hydrolysed cytosolic extracts from 24-hour cultures of RPTEC/TERT1 are shown for cells exposed to: cisplatin (9 mg L^{-1}) (i); cisplatin (9 mg L^{-1}) and Ch-SeNPs (5 mg L^{-1} of Se) (j); cisplatin (9 mg L^{-1}) and SeMet (5 mg L^{-1} of Se) (k).

MeSeCys (Fig. 8**e**). Besides, some studies have proposed that SeNPs could be precursors for SeCys synthesis without a previous oxidation to Se(IV) [43]. Therefore, our results confirm that internalised SeNPs enter cellular metabolism, although some of them seem to be released by exocytosis (**Section 3.3**).

Regarding cultures with SeMet, this was the major selenocompound in the corresponding cell extracts (Fig. 8**g**). On the contrary, no presence of this selenoamino acid was observed in the rest of the cases, in consonance with the poor efficiency of human cells to generate it [44]. An increase in $(SeCys)_2$ and MeSeCys peaks was also detected after SeMet treatment (Fig. 8**g**), but to a lesser extent than in extracts with Ch-SeNPs (Fig. 8**e**). Although the peak at 2 min could correspond not only to $(SeCys)_2$ but also to co-eluting SeOMet, the enhanced synthesis of SeCys caused by SeMet administration was confirmed by the higher intensity of MeSeCys peak (Fig. 8**g**). This is in agreement with the expected ability of mammalian cells to metabolise SeMet through *trans*-selenation giving rise to SeCys, which is further transformed into selenide by the β-lyase reaction [45,46]. However, AEC results show that only a very limited selenoamino acid conversion occurred, with most of SeMet remaining intact (Fig. 8**g**). This could be explained by the use of racemic DL-SeMet instead of the pure L-form, as cellular metabolism of D-SeMet is much less efficient [47]. On the other hand, the disruptive effect of cisplatin over the uptake of SeNPs and SeMet (**Section 3.4**) was demonstrated again, as an overall decrease in the intensity of Se peaks in the hydrolysed extracts occurred with the concomitant treatment of the Pt-drug and both selenocompounds (Fig. 8**f, 8h**). The results obtained after SEC and AEC analysis of HeLa extracts (data not shown) were very similar than those shown for RPTEC/TERT1, suggesting no differences between these cell lines in terms of metabolism of SeMet and SeNPs.

Pt was also monitored in the different extracts by AEC-ICP-MS as shown in Fig. 8**i-k**. No significant changes were observed regardless cisplatin was administered alone or in the presence of Ch-SeNPs or SeMet, showing a similar profile of cytosolic Pt in all cases. Likewise, there were no signs of preferential platination of SeMet or the presence of new platinated species in cells co-incubated with cisplatin and this amino acid (Fig. 8**k**), in contrast to the observations of García-Sar et al in rats [12], where they found Pt-SeMet adducts both in kidney extracts and in urine. Therefore, the absence of such complexes in the cytosolic samples analysed herein could be explained by their release from cells once formed, which would also be in consonance with the decrease in cisplatin uptake caused by SeMet (**Section 3.4**). This may suggest a mechanism to specifically remove Pt-SeMet adducts, as has been proposed in similar cases such as the release of Pt-GSH complexes through the GS-X pump [7].

Considering the above AEC results, both Ch-SeNPs and SeMet seem to stimulate the production of SeCys to a different extent. As SeCys is the only selenoamino acid included in the genetic code with its own codon (UGA), their increased levels may be related to the higher presence of

cellular selenoproteins found in SEC analysis (Fig. 7**e, 7f**). Nevertheless, these biomolecules could be originated not only by specific co-translational incorporation of SeCys during protein synthesis, but also through non-specific insertion of SeMet replacing Met in the nascent protein chain [41]. This may explain the increase in the proportion of high-molecular weight selenoproteins after SeMet treatment in spite of its poor conversion into SeCys, in contrast to the metabolism observed for SeNPs (Fig. 7**e, 7f and** Fig. 8**e, 8g**). However, although the levels of SeMet in SeMet-treated cells were significantly higher than the levels of $(SeCys)_2$ and MeSeCys in SeNP-treated ones (Fig. 8**e, 8g**), the first showed a lower production of selenoproteins (Fig. 7**e, 7f**). Thus, the synthesis based on the incorporation of SeMet seems to be less efficient, suggesting that a high proportion of internalised SeMet would remain free and not as part of proteins.

Although the current knowledge about Se-proteins is still limited, they are often involved in important biological functions such as redox homeostasis or antioxidant defense [42]. Thus, SeNPs and SeMet would enhance the redox status in healthy cells not only due to their own antioxidant properties but also through the induction of selenoprotein overexpression, which could be an additional benefit for nephroprotection. Moreover, this would be reinforced by an increase in the activity of other essential proteins to prevent oxidative damage such as glutathione peroxidase (GPx), superoxide dismutase (SOD) and catalase, which are known to be stimulated after Se administration [48].

4. Conclusions

The nephroprotective potential of Ch-SeNPs and SeMet has been evaluated for cisplatin-based antitumour therapies using RPTEC/TERT1 and HeLa cell models and a combination of bioanalytical techniques. ICP-MS analysis revealed that the presence of SeMet reduces the amount of both internalised cisplatin and Pt-DNA adducts, which may at least partially explain the slightly higher survival rates of kidney cells.

In contrast, Ch-SeNPs have no influence on the uptake of cisplatin and its binding to nuclear DNA, but its concomitant application produces a synergistic enhancement of the anticancer activity. Such aspect could also be an advantage from a renoprotective point of view, as lower doses of the Pt-drug would be required to achieve similar or even better results in terms of pharmacological efficacy, with the consequent decrease in kidney damage.

Both Ch-SeNPs and SeMet can be metabolised after their internalisation and favour an overexpression of cellular selenoproteins, as shown by SEC and AEC analysis. Thereby, as most of these biomolecules have antioxidant functions, this could be an additional benefit in order to revert the oxidative stress induced by cisplatin, which is one of the main causes of its nephrotoxicity.

Despite much more research is necessary to confirm and extend these preliminary results, Ch-SeNPs and SeMet are demonstrated to offer different but interesting characteristics to be considered as potential coadjuvants in future treatments to improve cisplatin efficacy and safety.

CRediT authorship contribution statement

Alejandro Iglesias-Jiménez: Writing – original draft, Visualization, Validation, Methodology, Investigation, Formal analysis, Conceptualization. **Gema Artiaga:** Methodology, Investigation. **Estefanía Moreno-Gordaliza:** Writing – review & editing, Supervision, Methodology, Conceptualization. **M. Milagros Gómez-Gómez:** Writing – review & editing, Supervision, Resources, Project administration, Methodology, Funding acquisition, Conceptualization.

Declaration of competing interest

The authors declare that they have no known competing financial interests or personal relationships that could have appeared to influence the work reported in this paper.

Acknowledgements

This work was supported by the Spanish Ministry of Science, Innovation and Universities (grant number PID2020-116067RB-100/AEI/10.13039/50110001103). A. Iglesias-Jiménez and G. Artiaga thank the Spanish Ministry of Education, Culture and Sports for their Predoctoral Fellowships (FPU 14/01412 and FPU 13/01693, respectively).

Data availability

Data will be made available on request.

References

[1] S. Ghosh, Cisplatin: The first metal based anticancer drug, Bioorg. Chem. 88 (2019) 102925, https://doi.org/10.1016/j.bioorg.2019.102925.
[2] D. Esteban-Fernández, E. Moreno-Gordaliza, B. Cañas, M.A. Palacios, M.M. Gómez-Gómez, Analytical methodologies for metallomics studies of antitumor Pt-containing drugs, Metallomics 2 (1) (2010) 19–38, https://doi.org/10.1039/b911438f.
[3] Z.Y. Duan, G.Y. Cai, J.J. Li, X.M. Chen, Cisplatin-induced renal toxicity in elderly people, Ther. Adv. Med. Oncol. 12 (2020) 175883, https://doi.org/10.1177/1758835920923430.
[4] S. Dasari, P. Bernard Tchounwou, Cisplatin in cancer therapy: Molecular mechanisms of action, Eur. J. Pharmacol. 740 (2014) 364–378, https://doi.org/10.1016/j.ejphar.2014.07.025.
[5] S. Camano, A. Lazaro, E. Moreno-Gordaliza, A.M. Torres, C. De Lucas, B. Humanes, J.A. Lazaro, M.M. Gomez-Gomez, L. Bosca, A. Tejedor, Cilastatin attenuates cisplatin-induced proximal tubular cell damage, J. Pharmacol. Exp. Ther. 334 (2) (2010) 419–429, https://doi.org/10.1124/jpet.110.165779.
[6] E. Moreno-Gordaliza, C. Giesen, A. Lázaro, D. Esteban-Fernández, B. Humanes, B. Cañas, U. Panne, A. Tejedor, N. Jakubowski, M.M. Gómez-Gómez, Elemental bioimaging in kidney by LA-ICP-MS as a tool to study nephrotoxicity and renal protective strategies in cisplatin therapies, Anal. Chem 83 (2011) 7933–7940, https://doi.org/10.1021/ac201933x.
[7] G. Artiaga, A. Iglesias-Jiménez, E. Moreno-Gordaliza, M.L. Mena, M.M. Gómez-Gómez, Differences in binding kinetics, bond strength and adduct formation between Pt-based drugs and S- or N-donor groups: A comparative study using mass spectrometry techniques, Eur. J. Pharm. Sci. 132 (2019) 96–105, https://doi.org/10.1016/j.ejps.2019.03.002.
[8] N. Pabla, Z. Dong, Cisplatin nephrotoxicity: Mechanisms and renoprotective strategies, Kidney Int. 73 (9) (2008) 994–1007, https://doi.org/10.1038/sj.ki.5002786.
[9] N.A.G. Dos Santos, M.A.C. Rodrigues, N.M. Martins, A.C. Dos Santos, Cisplatin-induced nephrotoxicity and targets of nephroprotection: An update, Arch. Toxicol. 86 (8) (2012) 1233–1250, https://doi.org/10.1007/s00204-012-0821-7.
[10] S. Li, X. He, L. Ruan, T. Ye, Y. Wen, Z. Song, S. Hu, Y. Chen, B. Peng, S. Li, Protective effect of mannitol on cisplatin-induced nephrotoxicity: a systematic review and meta-analysis, Front. Oncol. 11 (2021) 804685, https://doi.org/10.3389/fonc.2021.804685.
[11] M. Rao, M.N.A. Rao, Protective effects of selenomethionine against cisplatin-induced renal toxicity in mice and rats, J. Pharm. Pharmacol. 50 (6) (1998) 687–691, https://doi.org/10.1111/j.2042-7158.1998.tb06906.x.
[12] D. García Sar, M. Montes-Bayón, E. Blanco González, L.M. Sierra Zapico, A. Sanz-Medel, Reduction of cisplatin-induced nephrotoxicity in vivo by selenomethionine: The effect on Cisplatin - DNA adducts, Chem. Res. Toxicol. 24 (6) (2011) 896–904, doi: 10.1021/tx200085n.
[13] A. Khurana, S. Tekula, M.A. Saifi, P. Venkatesh, C. Godugu, Therapeutic applications of selenium nanoparticles, Biomed. Pharmacother. 111 (2019) 802–812, https://doi.org/10.1016/j.biopha.2018.12.146.
[14] H.W. Tan, H.Y. Mo, A.T.Y. Lau, Y.M. Xu, Selenium species: Current status and potentials in cancer prevention and therapy, Int. J. Mol. Sci. 20 (1) (2019) 75, https://doi.org/10.3390/ijms20010075.
[15] C. Ferro, H.F. Florindo, H.A. Santos, Selenium nanoparticles for biomedical applications: from development and characterization to therapeutics, Adv. Healthc. Mater. 10 (16) (2021) 2100598, https://doi.org/10.1002/adhm.202100598.
[16] S. Menon, K.S. Shrudhi Devi, R. Santhiya, S. Rajeshkumar, S. Venkat Kumar, Selenium nanoparticles: A potent chemotherapeutic agent and an elucidation of its mechanism, Colloids Surfaces B Biointerfaces 170 (2018) 280–292, https://doi.org/10.1016/j.colsurfb.2018.06.006.
[17] K. Bai, B. Hong, J. He, Z. Hong, R. Tan, Preparation and antioxidant properties of selenium nanoparticles-loaded chitosan microspheres, Int. J. Nanomedicine 12 (2017) 4527–4539, https://doi.org/10.2147/IJN.S129958.
[18] L. Shang, K. Nienhaus, G.U. Nienhaus, Engineered nanoparticles interacting with cells: size matters, J. Nanobiotechnol. 12 (5) (2014) 1–11, https://doi.org/10.1007/s12645-013-0033-8.
[19] F. Yang, Q. Tang, X. Zhong, Y. Bai, T. Chen, Y. Zhang, Y. Li, W. Zheng, Surface decoration by Spirulina polysaccharide enhances the cellular uptake and

anticancer efficacy of selenium nanoparticles, Int. J. Nanomed. 7 (2012) 835–844, https://doi.org/10.2147/IJN.S28278.
[20] M. Kieliszek, B. Lipinski, S. Błazejak, Application of sodium selenite in the prevention and treatment of cancers, Cells 6 (4) (2017) 39, https://doi.org/10.3390/cells6040039.
[21] J. S. Zheng, S.Y. Zheng, Y.B. Zhang, B. Yu, W. Zheng, F. Yang, T. Chen., Sialic acid surface decoration enhances cellular uptake and apoptosis-inducing activity of selenium nanoparticles, Colloids Surfaces B Biointerfaces 83 (1) (2011) 183–187, doi: 10.1016/j.colsurfb.2010.11.023.
[22] H. Wu, H. Zhu, X. Li, Z. Liu, W. Zheng, T. Chen, B. Yu, K.-H. Wong, Induction of apoptosis and cell cycle arrest in A549 human lung adenocarcinoma cells by surface-capping selenium nanoparticles: An effect enhanced by polysaccharide-protein complexes from Polyporus rhinocerus, J. Agric. Food Chem. 61 (41) (2013) 9859–9866, https://doi.org/10.1021/jf403564s.
[23] B. Afzal, D. Yasin, H. Naaz, N. Sami, A. Zaki, M.A. Rizvi, R. Kumar, P. Srivastava, T. Fatma, Biomedical potential of Anabaena variabilis NCCU-441 based Selenium nanoparticles and their comparison with commercial nanoparticles, Sci. Rep. 11 (1) (2021) 13507, https://doi.org/10.1038/s41598-021-91738-7.
[24] S. Lee, A. Shanti, Effect of exogenous pH on cell growth of breast cancer cells, Int. J. Mol. Sci. 22 (18) (2021) 9910, https://doi.org/10.3390/ijms22189910.
[25] H. Luo, F. Wang, Y. Bai, T. Chen, W. Zheng, Selenium nanoparticles inhibit the growth of HeLa and MDA-MB-231 cells through induction of S phase arrest, Colloids Surf. B Biointerfaces 94 (2012) 304–308, https://doi.org/10.1016/j.colsurfb.2012.02.006.
[26] B. Humanes, A. Lazaro, S. Camano, E. Moreno-Gordaliza, J.A. Lazaro, M. Blanco-Codesido, J.M. Lara, A. Ortiz, M.M. Gómez-Gómez, P. Martín-Vasallo, A. Tejedor, Cilastatin protects against cisplatin-induced nephrotoxicity without compromising its anticancer efficiency in rats, Kidney Int. 82 (6) (2012) 652–663, https://doi.org/10.1038/ki.2012.199.
[27] J. Xu, D.A. Gewirtz, Is autophagy always a barrier to cisplatin therapy? Biomolecules 12 (3) (2022) 463, https://doi.org/10.3390/biom12030463.
[28] N. Martinho, T.C.B. Santos, H.F. Florindo, L.C. Silva, Cisplatin-membrane interactions and their influence on platinum complexes activity and toxicity, Front. Physiol. 9 (2019) 1898, https://doi.org/10.3389/fphys.2018.01898.
[29] B. Toubhans, N. Alkafri, M. Quintela, D.W. James, C. Bissardon, S. Gazze, F. Knodel, O. Proux, A.T. Gourlan, P. Rathert, S. Bohic, D. Gonzalez, L.W. Francis, L. Charlet, R.S. Conlan, Selenium nanoparticles modulate histone methylation via lysine methyltransferase activity and S-adenosylhomocysteine depletion, Redox Biol. 61 (2023) 102641, https://doi.org/10.1016/j.redox.2023.102641.
[30] A.V. Shubin, I.V. Demidyuk, A.A. Komissarov, L.M. Rafieva, S.V. Kostrov, Cytoplasmic vacuolization in cell death and survival, Oncotarget 7 (34) (2016) 55863–55889, https://doi.org/10.18632/oncotarget.10150.
[31] M. Takano, N. Nakanishi, Y. Kitahara, Y. Sasaki, T. Murakami, J. Nagai, Cisplatin-induced inhibition of receptor-mediated endocytosis of protein in the kidney, Kidney Int. 62 (5) (2002) 1707–1717, https://doi.org/10.1046/j.1523-1755.2002.00623.x.
[32] P. Frisk, A. Yaqob, K. Nilsson, J. Carlsson, U. Lindh, Uptake and retention of selenite and selenomethionine in cultured K-562 cells, Biometals 13 (3) (2000) 209–215, https://doi.org/10.1023/A:1009272331985.
[33] J. Moon, I. Kitty, K. Renata, S. Qin, F. Zhao, W. Kim, DNA damage and its role in cancer therapeutics, Int. J. Mol. Sci. 24 (5) (2023) 4741, https://doi.org/10.3390/ijms24054741.
[34] R.J. Parker, A. Eastman, F. Bostick-Bruton, E. Reed, Acquired cisplatin resistance in human ovarian cancer cells is associated with enhanced repair of cisplatin-DNA lesions and reduced drug accumulation, J. Clin. Invest. 87 (3) (1991) 772–777, https://doi.org/10.1172/JCI115080.
[35] A. Galé, L. Hofmann, N. Lüdi, M.N. Hungerbühler, C. Kempf, J.T. Heverhagen, H. von Tengg-Kobligk, P. Broekmann, N. Ruprecht, Beyond single-cell analysis of metallodrugs by ICP-MS: Targeting cellular substructures, Int. J. Mol. Sci. 22 (17) (2021) 9468, https://doi.org/10.3390/ijms22179468.
[36] L. Amable, J. Fain, E. Gavin, E. Reed, Gli1 contributes to cellular resistance to cisplatin through altered cellular accumulation of the drug, Oncol. Rep. 32 (2) (2014) 469–474, https://doi.org/10.3892/or.2014.3257.
[37] E.G. Varlamova, M.V. Goltyaev, V.N. Mal'tseva, E.A. Turovsky, R.M. Sarimov, A. V. Simakin, S.V. Gudkov, Mechanisms of the cytotoxic effect of selenium nanoparticles in different human cancer cell lines, Int. J. Mol. Sci. 22 (15) (2021) 7798, https://doi.org/10.3390/ijms22157798.
[38] L. Guo, J. Xiao, H. Liu, H. Liu, Selenium nanoparticles alleviate hyperlipidemia and vascular injury in ApoE-deficient mice by regulating cholesterol metabolism and reducing oxidative stress, Metallomics 12 (2) (2020) 204–217, https://doi.org/10.1039/c9mt00215d.
[39] T. Liu, L. Xu, L. He, J. Zhao, Z. Zhang, Q. Chen, T. Chen, Selenium nanoparticles regulates selenoprotein to boost cytokine-induced killer cells-based cancer immunotherapy, Nano Today 35 (2020) 100975, https://doi.org/10.1016/j.nantod.2020.100975.
[40] J. Chen, Y. Zhang, Y. Lv, M. Tian, J. You, F. Chen, S. Zhang, W. Guan, Effects of selenomethionine on cell viability, selenoprotein expression and antioxidant function in porcine mammary epithelial cells, Front. Nutr. 8 (2021) 1–10, https://doi.org/10.3389/fnut.2021.665855.
[41] A.P. Kipp, J. Frombach, S. Deubel, R. Brigelius-Flohé, Selenoprotein W as biomarker for the efficacy of selenium compounds to act as source for selenoprotein biosynthesis, Methods Enzymol. 527 (2013) 87–112, https://doi.org/10.1016/B978-0-12-405882-8.00005-2.
[42] W.B. Minich, Selenium metabolism and biosynthesis of selenoproteins in the human body, Biochem. 87 (2022) S168–S177, https://doi.org/10.1134/S0006297922140139.
[43] G. Zhao, X. Wu, P. Chen, L. Zhang, C.S. Yang, J. Zhang, Selenium nanoparticles are more efficient than sodium selenite in producing reactive oxygen species and hyper-accumulation of selenium nanoparticles in cancer cells generates potent therapeutic effects, Free Radic. Biol. Med. 126 (2018) 55–66, https://doi.org/10.1016/j.freeradbiomed.2018.07.017.
[44] G.N. Schrauzer, Selenomethionine: A review of its nutritional significance, metabolism and toxicity, J. Nutr. 130 (7) (2000) 1653–1656, https://doi.org/10.1093/jn/130.7.1653.
[45] K.T. Suzuki, C. Doi, N. Suzuki, Metabolism of ^{76}Se-methylselenocysteine compared with that of ^{77}Se-selenomethionine and ^{82}Se-selenite, Toxicol. Appl. Pharmacol. 217 (2) (2006) 185–195, https://doi.org/10.1016/j.taap.2006.09.006.
[46] C.M. Weekley, J.B. Aitken, S. Vogt, L.A. Finney, D.J. Paterson, M.D. de Jonge, D. L. Howard, I.F. Musgrave, H.H. Harris, Uptake, distribution, and speciation of selenoamino acids by human cancer cells: X-ray absorption and fluorescence methods, Biochemistry 50 (10) (2011) 1641–1650, https://doi.org/10.1021/bi101678a.
[47] D. Kuehnelt, N. Kienzl, P. Traar, N.H. Le, K.A. Francesconi, T. Ochi, Selenium metabolites in human urine after ingestion of selenite, L-selenomethionine, or DL-selenomethionine: A quantitative case study by HPLC/ICPMS, Anal. Bioanal. Chem. 383 (2) (2005) 235–246, https://doi.org/10.1007/s00216-005-0007-8.
[48] E.A. Turovsky, A.S. Baryshev, E.Y. Plotnikov, Selenium nanoparticles in protecting the brain from stroke: possible signaling and metabolic mechanisms, Nanomaterials 14 (2) (2024) 1–23, https://doi.org/10.3390/nano14020160.